

## Article

# Nanocrystal-Based Topical Gels for Improving Wound Healing Efficacy of Curcumin

Vinith Kotian <sup>1,\*</sup>, Marina Koland <sup>1,\*</sup>  and Srinivas Mutalik <sup>2</sup> 

<sup>1</sup> Department of Pharmaceutics, NGSIM Institute of Pharmaceutical Sciences (NGSIMIPS), Nitte (Deemed to be University), Deralakatte, Mangalore 575018, India

<sup>2</sup> Department of Pharmaceutics, Manipal College of Pharmaceutical Sciences, Manipal Academy of Higher Education, Manipal 576104, India

\* Correspondence: marinakol@nitte.edu.in; Tel.: +91-988-604-2035

**Abstract:** Topical curcumin shows poor local availability because of its low aqueous solubility and inadequate tissue absorption. Curcumin nanocrystals were prepared by sonoprecipitation followed by lyophilization to improve surface area and solubility. The formulation was optimized by the Design of Experiment (DoE) approach. The nanocrystals were characterized for particle size, zeta potential, polydispersity index, scanning electron microscopy (SEM), powder x-ray diffraction (PXRD), practical yield and in vitro drug release studies. The nanocrystal-incorporated gel was evaluated for drug content, ex vivo permeation, in vivo skin irritation, and in vivo wound healing activity. Time of sonication and amplitude influenced the optimization of curcumin nanocrystals, but the effect of stabilizer concentrations was not significant beyond 0.5% w/w. SEM images of curcumin nanocrystals revealed irregular and plate-shaped particles with rough surfaces. PXRD patterns of curcumin nanocrystals showed low crystallinity compared to unprocessed curcumin powder. An in vitro drug release study demonstrated significant improvement in the percentage cumulative drug release in the form of nanocrystals compared to the unprocessed curcumin, and the release profile exhibited first-order kinetics. Curcumin nanocrystal gel showed 93.86% drug content and was free of skin irritation potential. Excision wound healing activity in albino rats showed that the curcumin nanocrystal gel exhibited significantly faster wound contraction than curcumin powder-incorporated gel.

**Keywords:** curcumin; nanocrystals; wound healing; topical delivery



**Citation:** Kotian, V.; Koland, M.; Mutalik, S. Nanocrystal-Based Topical Gels for Improving Wound Healing Efficacy of Curcumin. *Crystals* **2022**, *12*, 1565. <https://doi.org/10.3390/cryst12111565>

Academic Editors: Mohammed Rafi Shaik, Syed Farooq Adil and Mujeeb Khan

Received: 30 September 2022

Accepted: 28 October 2022

Published: 3 November 2022

**Publisher's Note:** MDPI stays neutral with regard to jurisdictional claims in published maps and institutional affiliations.



**Copyright:** © 2022 by the authors. Licensee MDPI, Basel, Switzerland. This article is an open access article distributed under the terms and conditions of the Creative Commons Attribution (CC BY) license (<https://creativecommons.org/licenses/by/4.0/>).

## 1. Introduction

The delivery of drugs via the skin is an essential route of administration for both topical and transdermal routes. Skin acts as a barrier or pathway to transport the drug to the desired site for transdermal formulations; whereas for topical formulations the skin is the target site [1]. Conventional topical formulations have been found to be time-consuming, complicated and uncomfortable, with low permeability and therapeutic efficacy resulting in poor bioavailability.

Recent years have seen a rapid growth in research in herbal-based drug delivery systems. Various herbal drugs such as silymarin, neem, curcumin, quercetin, and others, have been studied extensively as alternatives to conventional drugs due to rise in the cost of the manufacture of the latter, environmental issues with respect to the use of organic solvent, poor supply, and side effects [2].

Curcumin is a constituent from the rhizomes of *Curcuma longa* of the family Zingiberaceae and is known as a “cleanser of the body”. Curcumin has been reported to possess antioxidant, anti-inflammatory, antiviral, antifungal and antibacterial properties. It has been found to be effective against various diseases [3].

In earlier research, curcumin exhibited wound-healing properties which also decreased inflammation and stimulated cell proliferation, thus helping to reconstruct damaged tissue.

The anti-inflammatory, anti-infectious and antioxidant activities of curcumin are claimed to be responsible for its wound-healing properties. It has also been reported that curcumin improves cutaneous wound healing with a possible role in tissue remodeling, granulation, tissue formation, and collagen deposition. Curcumin enhances epithelial regeneration and increases fibroblast proliferation and vascular density when applied to topical wounds [4]. In vivo wound healing studies showed that curcumin improves dermal wound healing by reducing reactive oxygen species and lipid peroxidation [5]. It also possesses antioxidant, and anti-inflammatory activities that support wound healing through involvement in tissue remodeling, granulation, tissue forming, and collagen deposition [4].

Curcumin is a hydrophobic compound with poor solubility in aqueous media, making it unsuitable for topical application [5]. Previous studies have suggested that poor aqueous solubility would result in inadequate tissue absorption and degradation at alkaline pH, severely reducing its topical availability [5]. For poorly insoluble drugs, a reduction in particle size is the most favourable approach to increase solubility and dissolution rate by increasing the effective particle surface area. However, a reduction in the particle size to 'nano' dimensions is the most effective in increasing the saturation solubility of curcumin rather than micronization [6]. Drugs with nano dimensions can be used at lower concentrations and can lead to earlier onset of action. There is a dramatic shift in the physico-chemical properties as the drug's particle size is reduced to around 100 nm. This increases the surface area and solubility of the drug many-fold, and the bioavailability of the poorly soluble drug is improved proportionately [7].

Curcumin needs to have good skin penetrability. This depends on solubility and can be enhanced by preparing it as nanocrystals. Nanocrystals are pure solid drug particles with minimal amounts of additives such as stabilizers. These carrier-free submicron colloidal particles have a mean particle size in the nanometer range, typically between 10–800 nm. Stabilizers or surfactants are necessary for stabilization to minimize particle aggregation due to increased surface area and surface-free energy [8]. The large surface area of nanocrystals, available for dissolution due to their small particle size, is chiefly responsible for improving the bioavailability of poorly soluble drugs such as curcumin. Nanocrystals can also enhance penetration through the skin by accumulating in hair follicles, which can significantly contribute to dermal uptake [9].

Previous studies have reported using zinc oxide nanocrystals in combination with silver nanoparticles and *Ximenia americana* L. for wound healing applications, with a reduction in inflammation and enhancement of collagen fibre deposition in the skin lesions [10]. Other research involved using sodium alginate/cellulose nanocrystals loaded with  $\epsilon$ -polylysine for use as multifunctional wound dressings [11]. Another intriguing study assessed ultrasound-assisted reprecipitation as a highly effective technique for producing rod-like 7-ethyl-10-hydroxycamptothecin SN-38 nanocrystals [12].

In addition, skin penetration of curcumin can be boosted in dermatologic disorders because of inflammation and loss of the normal skin barrier function [13]. Besides having good skin permeability, nanocrystals can provide a drug concentration gradient across the skin sufficient to maintain continued passive diffusion and skin adhesion [14].

In our prior studies, we adequately synthesized curcumin nanocrystals using a modified nanoprecipitation technique to examine the tissue-protective properties of nanocrystal curcumin in mitigating testicular toxicity caused by cyclophosphamide [15]. Another recent work used the wet ball milling technique to synthesize nanocurcumin with a high positive surface charge by altering the ratio of CTAB and Pluronic F127. This nanocurcumin was shown to augment the antibacterial effect by destroying the bacterial cell surface [16].

The vehicle or base used for topical application can play an essential role in drug delivery, cutaneous availability and the wound healing process. Gels are mostly preferred for wound treatment because their soothing effect, and their ability to hold a large amount of water can help to supply dry wounds with sufficient moisture. They can also absorb excess discharge from wounds without interfering in the healing process. Gels prepared from polymers such as Carbopol are well tolerated by the skin [17]. Carbopol is a major

component of drug delivery gel systems for buccal, ocular and a dermatologic base for topical application. The rheological behaviour of carbopol gels do not change appreciably in the pH range of 5–8 [18]. Our investigation incorporated curcumin nanocrystals in a carbopol gel base for topical application.

This investigation aimed to develop a topical formulation of curcumin nanocrystals with enhanced skin permeability and superior wound healing by increasing the solubility of curcumin and its skin adhesion.

## 2. Materials and Methods

### 2.1. Materials

Curcumin, Carbopol, polyvinyl pyrrolidone (PVP) and ethanol were obtained from Loba Chemie, Pvt. Ltd., Mumbai, India. Methanol was procured from Nice chemicals Kerala, India. dimethyl sulphoxide (DMSO) was purchased from Hi-Media Laboratories Mumbai, India. All other chemicals used were of analytical or synthetic grade.

### 2.2. Preparation of Curcumin Nanocrystals

Nanocrystals were prepared by precipitation, a bottom-up method, followed by ultrasonication [19–21]. Curcumin was dissolved in 5 mL DMSO at room temperature. The solution was poured into 50 mL of distilled water as an anti-solvent containing the desired concentration of polyvinyl pyrrolidone (PVP) as a stabilizer, and subjected to sonication in an ice bath. The obtained nanosuspension was freeze-dried using D-mannitol as a cryoprotectant to obtain curcumin nanocrystals powder [22]. Based on a literature survey and trial batches, various critical process variables and formulation variables used for the sonoprecipitation were optimized using the Box-Behnken design with response surface methodology. The software, Design Expert 11.0.3.0 64-bit (Stat-Ease, Inc. Minneapolis, MN, USA) was used for optimization. Time of sonication, stabilizer concentration, and amplitude were independent variables. Responses related to particle size and practical yield as dependent variables were analyzed as shown in Table 1.

**Table 1.** Box—Behnken experimental design showing the factors and responses used for optimization.

Run	Factor 1 A: Conc. of Stabilizer (%)	Factor 2 B: Time of Sonication (min)	Factor 3 C: Amplitude ( $\mu\text{m}$ )	Response 1 Particle Size (nm)	Response 2 Practical Yield (%)
1	0.75	20	100	159	68
2	0.5	20	75	178	70
3	0.75	30	75	128	65
4	0.5	20	75	178	70
5	0.25	20	100	168	69
6	0.5	20	75	178	70
7	0.75	10	75	240	78
8	0.5	20	75	178	70
9	0.25	10	75	222	76
10	0.5	10	100	210	75
11	0.75	20	50	234	78
12	0.25	30	75	135	65
13	0.25	20	50	254	82
14	0.5	30	100	94	61
15	0.5	10	50	243	80
16	0.5	30	50	186	73
17	0.5	20	75	178	70

### 2.3. Determination of Morphology by Scanning Electron Microscopy (SEM)

Lyophilized formulations were assessed by JEOL-JSM 6380LA (JEOL, Tokyo, Japan), an analytical scanning electron microscope, to determine the particle size, surface topography, texture and morphology distribution. A sample of the nanosuspension after sonication and

before freeze-drying was also examined. The samples for SEM were prepared by lightly sprinkling the curcumin nanocrystal powder on a double side adhesive tape, which was stuck on an aluminum stub. The photomicrographs were then captured [23].

#### 2.4. Determination of Average Particle Size and Zeta Potential

The particle size, polydispersity index and zeta potential of curcumin nanocrystals were analyzed using a Zeta sizer (Nano ZS Malvern, UK). The particle size of the nanocrystals was measured by dynamic light scattering. The Zeta potential was determined by a combination of laser dropper velocimetry (DLV) and Phase Analysis Light Scattering (PALS) by a patented technique called M-3 PALS to measure the particle electrophoretic mobility [24]. In this technique, the charged particles were attracted to oppositely charged electrodes and their velocity was measured and expressed as electrophoretic mobility in unit field strength. The entire measurement was carried out at 25 °C.

#### 2.5. Percentage Yield

The percentage yield was calculated based on the weight of the nanocrystals obtained and mass of curcumin and polymers added [25].

$$\text{Percentage yield} = \frac{\text{Mass of nanocrystals obtained}}{\text{Total weight of drug and polymer}} \times 100 \quad (1)$$

#### 2.6. Powder X-ray Diffraction (PXRD) Studies

PXRD patterns were recorded by a Y2000 powder X-ray diffractometer (Dandong, China). The powder was placed in the sample slot and pressed smoothly with frosted glass. Then, the analysis was carried out with a scan speed at 0.04°/min, and the patterns were recorded over 2θ angle ranged from 5 °C to 80 °C [26].

#### 2.7. In Vitro Drug Release Studies

The in vitro release determination from pure or unprocessed curcumin and optimized nanocrystals was carried out in a USP Type II Dissolution Test Apparatus (Electrolab, Bangalore, India). Phosphate buffer (900 mL, pH 7.4) was taken as the dissolution medium at a stirring speed of 75 rpm at for 90 min. About 10 mg each of unprocessed curcumin powder or curcumin nanocrystals was subjected to dissolution studies. At predetermined time intervals, aliquots of 3 mL were withdrawn from the dissolution medium and replaced with equal volumes of fresh buffer into the glass vessel to preserve the constant volume. After appropriate dilution and filtration, the samples were analyzed using a UV/Visible spectrophotometer at a λ<sub>max</sub> of 436 nm [27].

#### Kinetic Analysis of Drug Release

Drug release data were analyzed using the software PCP-Disso-v3 (BVDU's Poona College of Pharmacy, Pune, India) to determine the kinetics of the drug release.

#### 2.8. Formulation of Nanocrystals-Based Gel

For the ex vivo and in vivo studies, we prepared a Carbopol gel base into which curcumin nanocrystals or plain curcumin powder was incorporated. To prepare the gel base, Carbopol 934P (2% w/w) was dispersed in water, stirred for 2 h and kept overnight for complete swelling. The pH was adjusted to 6.0 with triethanolamine. A sufficient quantity of the optimized curcumin nanocrystals was mixed in the gel base until homogeneous to obtain 1.0% w/w strength [28]. A similar gel was prepared with 1% w/w curcumin powder as well.

## 2.9. Evaluation of Nanocrystals-Based Gel

### 2.9.1. Drug Content

The curcumin content in the gel formulations was estimated by dispersing 1 g of curcumin nanocrystal gel in phosphate buffer pH 7.4 containing 3% Tween 80. The clear solution was diluted with 10 mL methanol and further diluted with the buffer. The absorbance was measured at 436 nm in a UV spectrophotometer [26].

### 2.9.2. Ex Vivo Drug Permeation Study

The institutional animal ethics committee (IAEC) approved the protocol for this study. Skin permeation studies were performed using a vertical-type diffusion cell, mounted with excised rat skin. Rats were sacrificed by a lethal injection of pentobarbitone. Hairs from the dorsal surface were removed using an animal hair clipper. Subcutaneous tissue was removed surgically, and the dermis side was wiped with isopropyl alcohol to remove adhered fat, then washed with phosphate-buffered saline (pH 7.4), and stored at  $-20\text{ }^{\circ}\text{C}$ . The excised skin was mounted between the donor and the receptor compartment of the diffusion cell. We placed a quantity of the formulation equivalent to 5 mg of curcumin nanocrystals in the donor compartment, while the receptor compartment was filled with 12 mL of phosphate buffer of pH 7.4 with 3% Tween 80 and maintained at  $37\text{ }^{\circ}\text{C}$  [29]. The contents of the receptor compartment were stirred by a magnetic stirrer at 100 rpm. An aliquot of 1 mL was withdrawn at suitable time intervals and replaced with the same volume of fresh buffer. Samples were analyzed by a UV spectrophotometer at 436 nm [30].

### 2.9.3. In Vivo Skin Irritability Study

Potential skin irritability of the nanocrystals was tested in Albino Wistar rats. Male Albino rats (5–6 weeks old; 150–200 g) were selected for the study. We utilized four groups of four rats each to determine the skin irritation potential of the formulation. The animals were divided into four groups as follows:

- Control (Untreated)
- Test 1 (FC-1 or unprocessed curcumin powder-containing gel, 1.0% w/w)
- Test 2 (FC-2b or optimized curcumin nanocrystal gel, 1.0% w/w) and
- Standard (Povidone Iodine Ointment USP, 5.0% w/w)

The fur on the dorsal area of the trunk of the experimental animals was removed with the help of a hair-removing cream. A 0.5 g of the optimized curcumin nanocrystal gel/curcumin powder-containing gel/povidone iodine ointment was applied to a surface area of about  $6\text{ cm}^2$  of the test group animals twice a day—morning and night—for seven days and covered with a cotton bandage. The animals were observed for any reaction after 24 h, 48 h, 72 h respectively for seven days after depilation. The exposed skin was evaluated by monitoring the formation of any possible oedema (grades 0–4) and erythema/eschar (grades 0–4) as the response criteria at specified time intervals [31].

### 2.9.4. Excision Wound Healing Study

Male rats weighing 180–200 g were taken and anesthetized with a combination of ketamine hydrochloride (40 mg/kg) and xylazine (10 mg/kg) via intraperitoneal injection and the dorsal surface of these animals were shaved [32]. The area in which the wound was to be created was marked using a permanent marker and the wound of a circular area of  $4.9\text{ cm}^2$  and depth of 0.2 cm was made using a surgical blade, toothed forceps and pointed sharp scissors. Throughout the study, the entire wound was left open. A preliminary study was carried out on rats to optimize the concentration of curcumin nanocrystal concentration required for faster wound healing. The two effective concentrations were 0.5 and 1.0% w/w of the optimized curcumin nanocrystals in the Carbopol gel base. For the final excision wound healing study, five groups of rats were used. Group I was left untreated and used as control. Animals in Group II, or standard, were treated with Povidone Iodine ointment USP (5% w/w), Group III with FC-1 or 1.0% curcumin powder-containing gel, Group IV

with FC-2a or 0.5% w/w of the curcumin nanocrystal-containing gel, and Group V with FC-2b or 1.0% curcumin nanocrystal-containing gel. All the treatments were applied once daily for 20 days. The wound area in all groups was measured on 1st, 4th, 7th, 10th, 15th and 20th days by tracing the wound on a transparent paper and area was calculated using 1 mm<sup>2</sup> graph paper. Change in the wound area was observed and the wound contraction was evaluated by using the following formula [33].

$$\% \text{ Wound Contaction} = \frac{\text{Healed area}}{\text{Total wound area}} \times 100 \quad (2)$$

$$\text{Healed area} = \text{Original wound area} - \text{Present wound area} \quad (3)$$

### 2.9.5. Statistical Analysis

The data from the treated groups were compared with the control group by applying statistical analysis using Graphpad Prism 8 Software (San Diego, CA, USA). The results were analyzed using one-way analysis of variance (ANOVA). A probability level of less than  $p < 0.05$  was considered statistically significant.

## 3. Results and Discussion

### 3.1. Preparation of Curcumin Nanocrystals by Sonoprecipitation Method

#### Optimization of Curcumin Nanocrystals

By preliminary experiments, the concentration of stabilizer, time of sonication and amplitude of sonication were identified as the most significant independent variables influencing the particle size and practical yield. The optimization of the experimental conditions was carried out as per the runs generated by the DesignExpert® software. Box-Behnken design along with Response surface method (RSM) was used in the optimization operated at three levels and three factors generating a total of 17 runs with five centre points. We selected the time of sonication (10 to 30 min) and stabilizer concentration (0.25 to 0.75% w/w of drug) as independent variables and particle size and practical yield (%) as dependent variables. The variables used for the Box-Behnken experimental design are shown in Table 1.

The 17 runs were formulated, their particle sizes were obtained using the Malvern zetasizer ZS, and practical yield was calculated. The data obtained were fed into the data table and further studied by using analysis of variance (ANOVA). For the suggested model, its Fisher variation ratio (F-value) and  $p$ -value were determined to indicate if the former was significant or not. A probability value ( $p$ -value) of less than 0.05 meant the significance of the model was at the 95% confidence level.

- Effect of variables on particle size of nanocrystals

The results for particle size of curcumin nanocrystals on applying ANOVA are given in Table 2. A model F-value of 52.82 implies the model is significant. There is only a 0.01% chance that an F-value this large could occur due to noise.  $p$ -values less than 0.05 indicate that the model terms are significant. In this case B, C, BC, A<sup>2</sup>, C<sup>2</sup> are significant model terms.  $p$ -values greater than 0.1000 indicate the model terms are not significant. The negative coefficients for A, B and C indicate that, with an increase in stabilizer concentration, time of sonication and amplitude, respectively, the particle size decreases. However, the effect of A or stabilizer concentration (greater than 0.5%) on particle size is not very significant ( $p$  value > 0.05). The coefficient estimate represents the expected change in response per unit change in factor value when all remaining factors are held constant. The intercept in an orthogonal design is the overall average response of all the runs. The coefficients are adjustments around that average based on the factor settings.

**Table 2.** Parameters generated from ANOVA for Particle Size (nm) and Practical Yield (%).

Factor	Particle Size			Practical Yield		
	F-Value	p-Value	Coefficient Estimate	F-Value	p-Value	Coefficient Estimate
Model	52.82	<0.0001	178.00 (Intercept)	33.98	<0.0001	70.00 (Intercept)
A—Conc. of stabilizer (%)	0.6349	0.4517	−2.250	0.6702	0.4400	−0.375
B—Time of sonication (min)	271.19	<0.0001	−46.50	150.80	<0.0001	−5.620
C—Amplitude (μm)	160.29	<0.0001	−35.75	119.15	<0.0001	−5.000
AB	2.45	0.1615	−6.250	0.5957	0.4655	−0.500
AC	0.4742	0.5132	2.750	1.34	0.2849	0.7500
BC	13.64	0.0077	−14.750	7.30	0.0306	−1.750
A <sup>2</sup>	9.31	0.0186	11.870	5.64	0.0492	1.500
B <sup>2</sup>	4.91	0.0622	−8.630	0.6271	0.4544	−0.500
C <sup>2</sup>	12.71	0.0092	13.880	18.97	0.0033	2.750

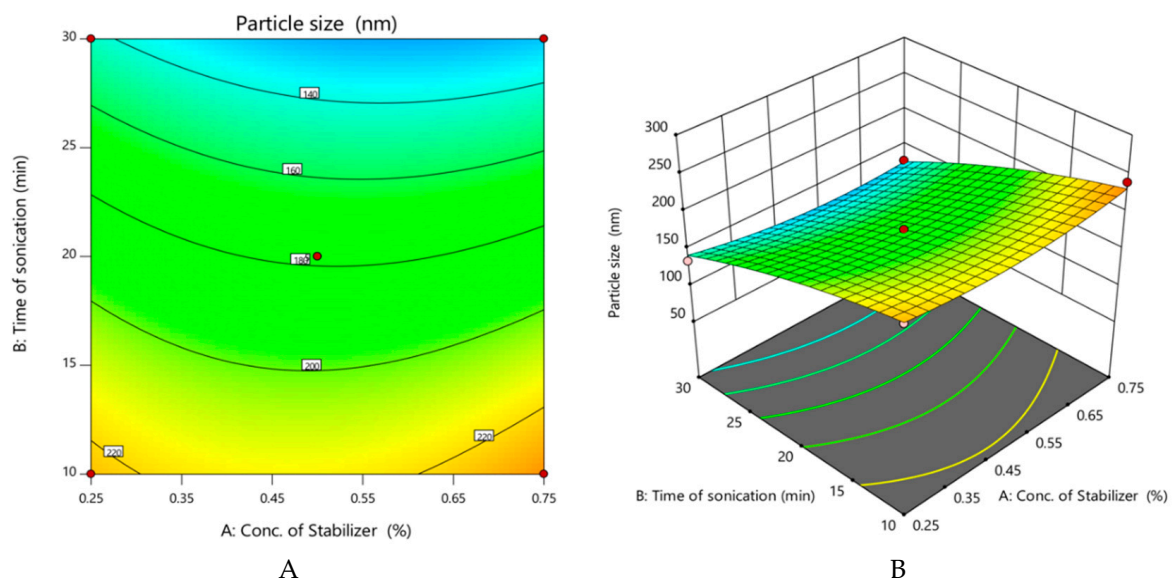
The final equation in terms of Coded Factors is:

$$\text{Particle size} = +178.00 - 2.25A - 46.50B^* - 35.75C^* - 6.25AB + 2.75AC - 14.75BC^* + 11.87A^2 - 8.63B^2 + 13.88C^2 \text{ where } '^*' \text{ represents significant factors.}$$

The final equation in terms of actual factors is obtained as:

$$\text{Particle size} = 423.625 + -182 \times \text{Conc. of stabilizer} + 4.475 \times \text{Time of sonication} + -3.8 \times \text{Amplitude} + -2.5 \times \text{Conc. of stabilizer} \times \text{Time of sonication} + 0.44 \times \text{Conc. of stabilizer} \times \text{Amplitude} + -0.059 \times \text{Time of sonication} \times \text{Amplitude} + 190 \times (\text{Conc. of stabilizer})^2 + -0.08625 \times (\text{Time of sonication})^2 + 0.0222 \times (\text{Amplitude})^2$$

The obtained regression model was used to draw the contour and 3D surface plots relating time of sonication and concentration of stabilizer to the particle size as shown in Figure 1.

**Figure 1.** Cont.

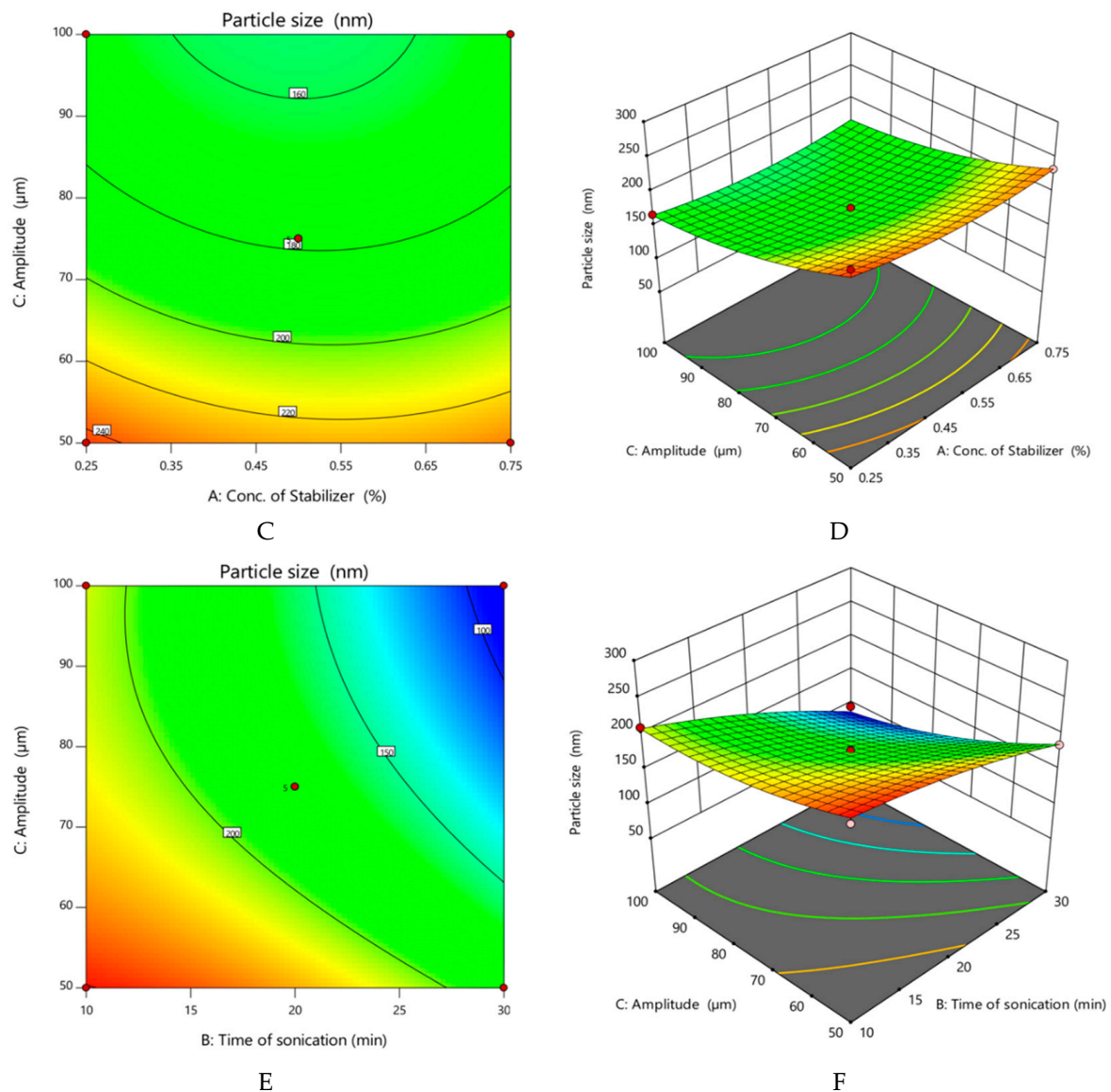


**Figure 1.** Effect of variables on particle size of curcumin nanocrystals. (A,B) Contour and 3D surface plots respectively of A or concentration of stabilizer (% w/v) versus B or time of sonication (min). (C,D) Contour and 3D surface plots respectively of A versus C or Amplitude ( $\mu\text{m}$ ). (E,F) Contour and 3D surface plots respectively of B versus C.

The 3D contour plot shows the variation in particle size with change in concentration of stabilizer, time of sonication and amplitude is explained with the colour-coded contours. The yellow and orange shades indicate regions of larger particle size, while the green and blue shades indicate regions of smaller particle size.

- Effect of variables on practical yield of nanocrystals

The results for the practical yield of curcumin nanocrystals on applying ANOVA are given in Table 2. The model F-value of 33.98 implies the model is significant, meaning there is only a 0.01% chance that a large F-value could occur due to noise.

As explained earlier,  $p$ -values less than 0.0500 mean that the model terms are significant. Hence B, C, BC,  $A^2$ ,  $C^2$  are significant model terms. As evident in Figure 2, the effect of time of sonication and amplitude on the practical yield is significant but not so in the case of Factor A or concentration of stabilizer, PVP. Further, increase in the stabilizer concentration beyond 0.5% w/v did not significantly ( $p > 0.05$ ) increase the practical yield.

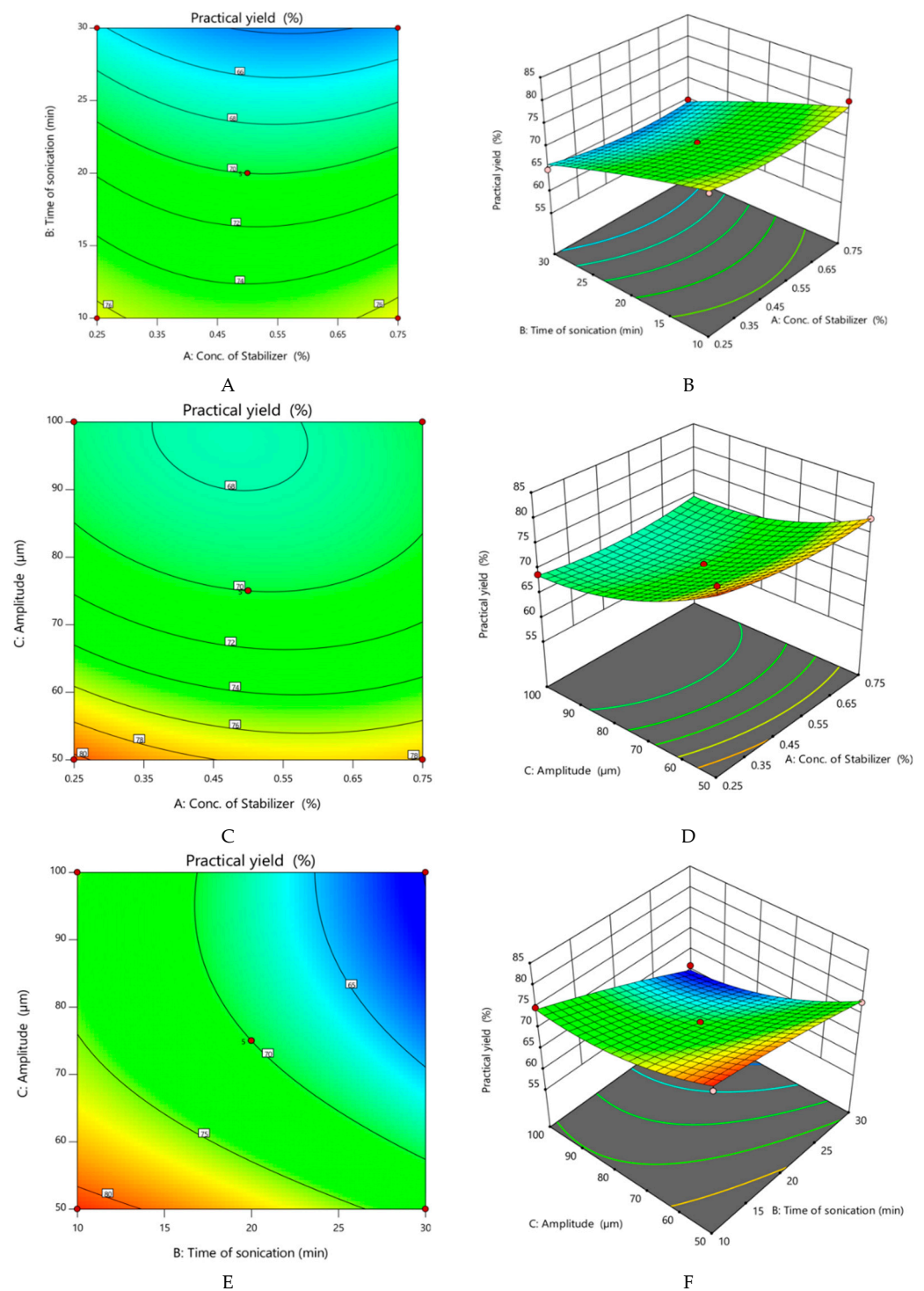


**Figure 2.** Effect of variables on practical yield of curcumin nanocrystals. (A,B) Contour and 3D surface plots respectively of A or concentration of stabilizer (% w/v) versus B or time of sonication (min). (C,D) Contour and 3D surface plots respectively of A versus C or Amplitude (μm). (E,F) Contour and 3D surface plots respectively of B versus C.

The final equation in terms of coded factors is:

$$\text{Practical yield} = 70 - 0.375A - 5.625B^* + -5C^* + -0.5AB + 0.75AC + -1.75BC^* + 1.5A^2 + -0.5B^2 + 2.75C^2$$

where '\*' represents significant factors.

The final equation in terms of actual factors is:

Practical yield =  $117.75 + -30.5 \times \text{Conc. of stabilizer} + 0.2625 \times \text{Time of sonication} + -0.78 \times \text{Amplitude} + -0.2 \times \text{Conc. of stabilizer} \times \text{Time of sonication} + 0.12 \times \text{Conc. of stabilizer} \times \text{Amplitude} + -0.007 \times \text{Time of sonication} \times \text{Amplitude} + 24 \times (\text{Conc. of stabilizer})^2 + -0.005 \times (\text{Time of sonication})^2 + 0.0044 \times (\text{Amplitude})^2$

The contour and 3D surface plots relating the concentration of stabilizer, time of sonication and amplitude of sonication to the practical yield is shown in Figure 2. As in the case of Figure 1, 3D contour plot shows the variation in practical yield with changes in these three parameters and is explained with the colour-coded contours. The yellow-shaded regions indicate higher yields.

- Numerical optimization

A numerical method was used to optimize and predict the best combination of independent variables to give better particle size and practical yield based on desirability. The goal for practical yield was adjusted to maximum and for particle size was in the range. The optimization of nanocrystals in terms of practical yield in the range of 61% to 82% and particle size in the range of 94 nm to 254 nm was carried out. The software generated 27 solutions, and the one that possessed desirability values (near to 1) was selected, which was 0.929. The percentage error was calculated by the software after conducting the experiments. The solution formula was formulated, and the result was found to be in agreement with the prediction made by the software with percentage error for particle size and practical yield.

The correlation chart between the observed experimental values and the predicted median clearly showed there was not much deviation between predicted and experimental values. The predicted values for particle size and practical yield of the nanocrystals were 178 nm and 70% respectively, while the actual values were 180.3 nm and 72%, respectively with a percentage error not exceeding 5.5%. Thus, we concluded that these values are within the range given by the suggested model. Then we formulated the optimized batch of curcumin nanocrystals (Batch 4) using 0.5% w/v of polyvinyl pyrrolidone as the stabilizer with 20 min of sonication time at an amplitude of 75  $\mu\text{m}$ , yielding the desired particle size and practical yield.

### 3.2. Particle Size, Polydispersity Index (PDI), Zeta Potential

The average particle size, PDI and zeta potential of the optimized Curcumin nanocrystals (Batch 4) determined using Malvern Zeta sizer Nanoseries, were found to be  $180.3 \pm 32.4$  nm,  $0.246 \pm 0.054$  and  $-39 \pm 0.34$  mV, respectively (Figure 3).

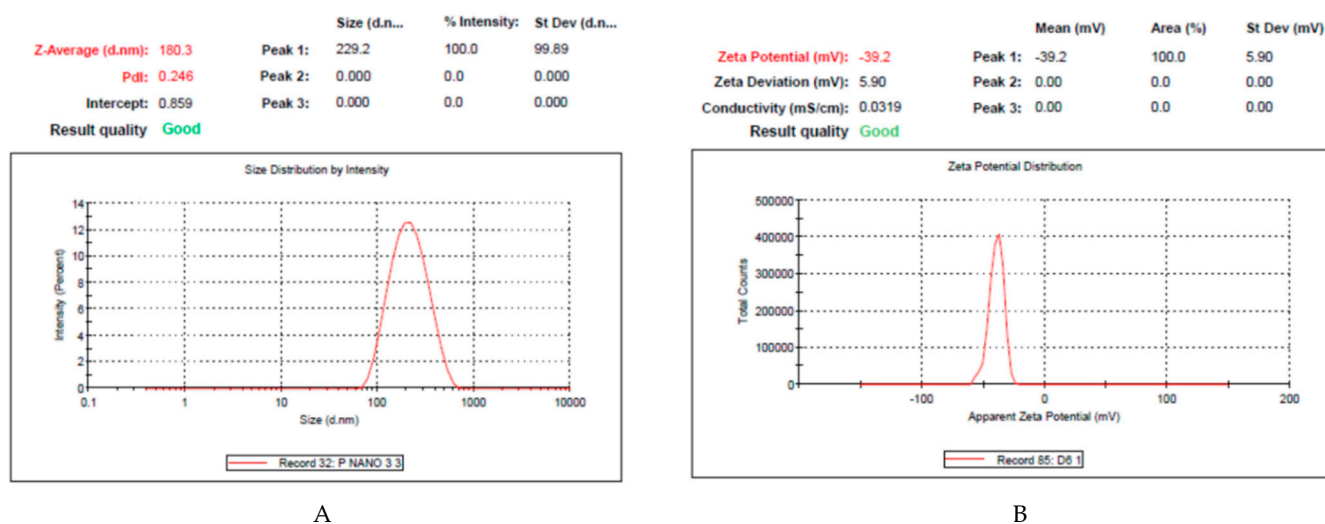


Figure 3. Results of particle size (A) and zeta potential (B) determinations of optimized nanocrystals.

As described earlier, particle size was primarily dependent on the time of sonication and amplitude, and the former decreased when the latter two factors were increased [34]. Initially, with increase in stabilizer concentration, particle size decreased but not significantly at concentrations above 0.5%. It was observed from the results obtained in terms of particle size that as the concentration of stabilizer increased, the particle size increased slightly, then as sonication time increased the size decreased [35].

Low values of PDI (<0.3) mean narrow size distribution of the dispersion, while higher magnitude of zeta potential values (−39 mV) indicate greater stability. Thus, the zeta potential is an essential physicochemical parameter that can influence nanosuspension stability [36]. Aggregation of the particles can be prevented when large repulsive forces are generated between particles with a similar electric charge. Such suspensions can also be easily redispersed [37].

### 3.3. Morphology Determination

The crystal habit and shape of particles are influenced largely by fabrication technology, additives, and lyophilization [38]. The surface morphology of the optimized curcumin nanocrystal was characterized by SEM before sonication and after lyophilization and is depicted in Figure 4. The nanosuspension obtained before ultrasonication was found to consist of irregular shaped larger particles (Figure 4A). After sonication and freeze drying of the nanosuspension of curcumin nanocrystals, there seemed to be a dramatic alteration in the particle size and shape. Irrespective of the concentration of stabilizer used, the curcumin nanocrystals were plate-shaped with rough surfaces, as evident in Figure 4B. Homayouni et al., also reported similarly shaped curcumin nanocrystals after freeze-drying [39]. The plate shape of the lyophilized nanocrystals could be attributed to the aggregation of rod-like crystals during the freeze-drying process. Nevertheless, these crystals were smaller in size when compared to those obtained before sonication. The plate shape crystal habit and size are typical of crystallized curcumin when prepared by antisolvent crystallization and sonication, followed by freeze drying of the nanosuspensions [39]. The greater surface area of these nanocrystals could be a deciding factor in improving their dissolution rate [40,41].

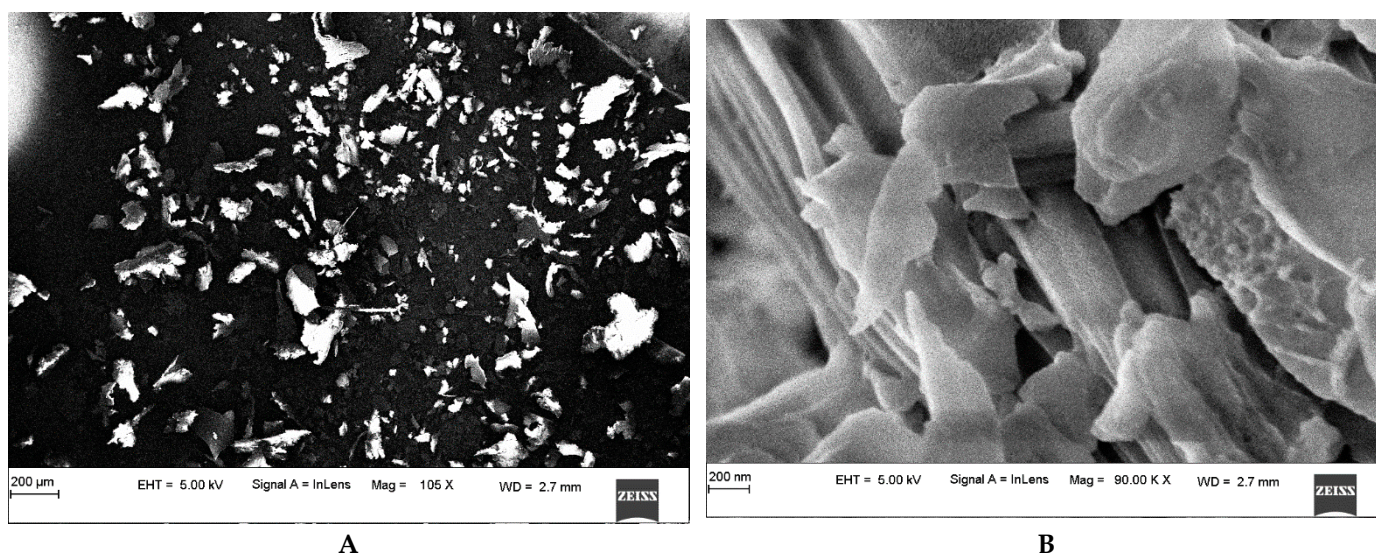


**Figure 4.** SEM image of optimized curcumin nanocrystals (Batch 4). (A) Before sonication; (B) After lyophilization.

### 3.4. Powder X-ray Diffraction Studies (PXRD)

X-ray diffraction was performed to investigate the crystallinity of the lyophilized nanocrystals of curcumin. A pattern is generated when X-rays interact with crystalline substances, known as a diffraction pattern. A diffraction pattern is unique for a specific

crystalline material. In a mixture of materials, each substance produces a diffraction pattern independently of the others. Bigger crystals produce narrow peaks, while broader peaks in the diffraction pattern mean that the crystal is smaller, or a defect is present in the crystalline structure, or that the sample might be amorphous in nature. Amorphous solids are considered to lack perfect crystallinity. The final shape of the X-ray diffraction pattern obtained is the effect of the total contribution by the sample (crystalline and amorphous), noise (background), and instrumental function. The crystalline contribution to the pattern by the nanocrystalline sample is made up of the elastic and inelastic scattering that can provide information of the particle size of the crystals, the amorphous region, and the background. Since it is impossible to separate the inelastic scattering contribution and the diffracted signal, it is difficult to determine the crystalline portion in the nanocrystals [42].

Figure 5 shows the X-ray diffraction pattern obtained for the unprocessed curcumin powder and optimized nanocrystals of curcumin (Batch 4). Unprocessed curcumin showed intense peaks in the PXRD pattern (Figure 5A). The patterns appear to be similar but with peaks of lower intensity in the case of the nanocrystals, probably due to the lesser crystallinity as a result of the amorphization of the latter. There is also a greater contribution from the background noise of the instrument as seen in Figure 5B. However, the presence of a few sharp peaks in Figure 5B indicates that curcumin nanocrystals are still crystalline and have not been completely amorphized. Thus, the formulation is a mixture of both amorphous and crystalline form of curcumin.

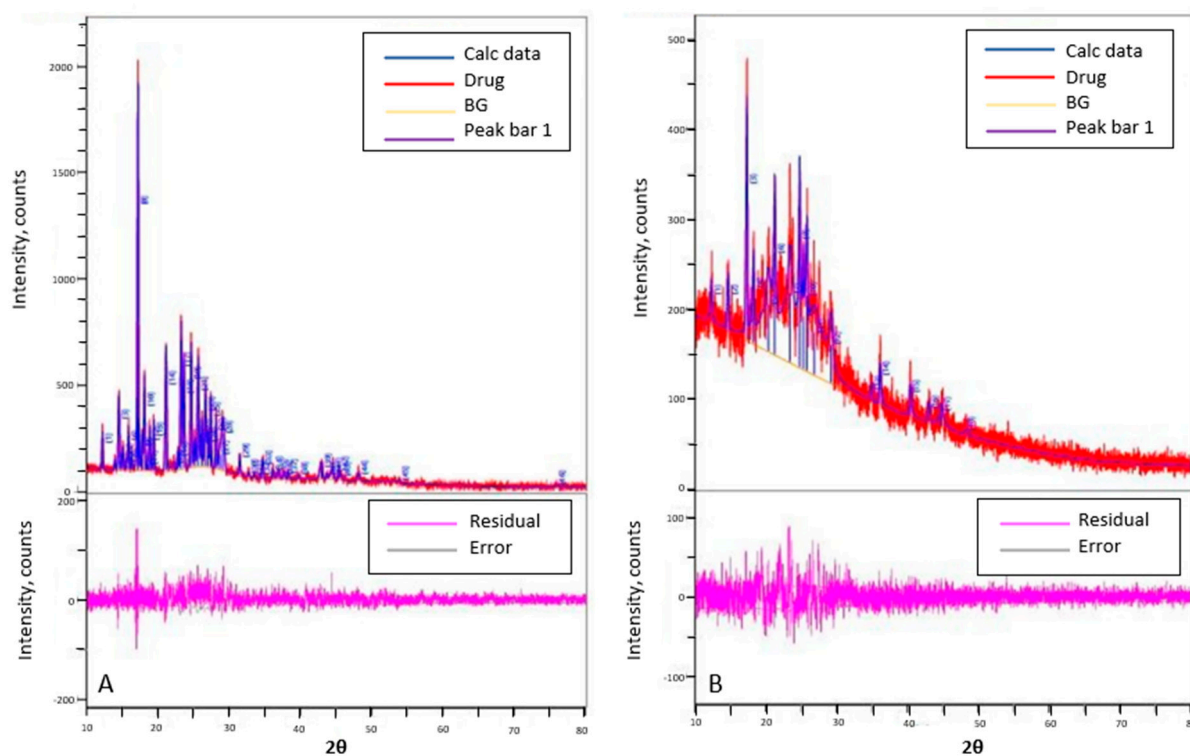


**Figure 5.** PXRD of unprocessed curcumin powder and its nanocrystals. (A) Unprocessed curcumin powder; (B) Optimized curcumin nanocrystals (Batch 4).

### 3.5. In Vitro Drug Release Studies

The release of curcumin from the optimized nanocrystal (F1) was found to be considerably more when compared to curcumin powder (F2). Figure 6 shows that 93.26% of curcumin was released from curcumin nanocrystals after 90 min, compared to just 25.10% from unprocessed curcumin powder. This confirms that nanocrystals enhance curcumin dissolution by its increased surface area due to the smaller size of its particles as compared to curcumin powder [38]. According to Noyes-Whitney equation, the dissolution rate of a

solid depends on the effective surface area, aqueous solubility and concentration gradient across the hydrodynamic diffusion layer. Hence when the particle size is reduced, as in the case of nanocrystals, the effective surface area is increased, diffusion layer thickness is decreased which increases the concentration gradient, resulting in an enhanced dissolution rate of the particles [43,44]. The hydrophilic nature of the stabilizer, polyvinyl pyrrolidone may also play a role by promoting wetting and dissolution of the lipophilic curcumin.

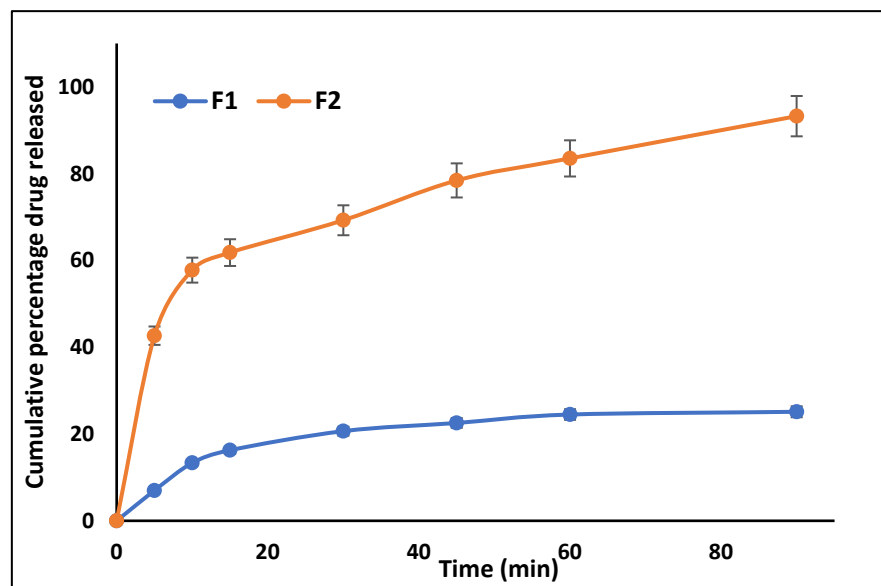


**Figure 6.** Drug release profile of unprocessed curcumin powder (F1) and curcumin nanocrystals (F2).

#### Kinetic Analysis of In Vitro Drug Release Studies

In vitro drug release study data were fitted to different models such as zero order and first order equations to predict the kinetics and drug release mechanism. The release profile of curcumin from the nanocrystal gel was found to follow first order kinetics ( $R^2 = 0.9908$ ) based on a greater regression coefficient value as compared to that of the zero-order model ( $R^2 = 0.9041$ ) [45].

#### 3.6. Evaluation of Nanocrystals Based Gel

##### 3.6.1. Drug Content in Nanocrystal-Incorporated Gel

Curcumin contents of the gel formulations of unprocessed curcumin powder (FC-1 containing 1.0% w/w of curcumin) and the gel containing 0.5% w/w curcumin nanocrystals (FC-2a) and 1.0% w/w curcumin nanocrystals (FC-2b) were estimated and the values were found to be  $93.86 \pm 0.13\%$ ,  $94.64 \pm 0.37\%$ , and  $95.00 \pm 0.23\%$ , respectively. The results also indicated that the drug was uniformly distributed throughout the gel base. Drug content uniformity plays an important role in the homogeneity of the dispersed drug in the formulation [46].

##### 3.6.2. Ex Vivo Drug Permeation Study

The permeation profiles of curcumin from the nanocrystal gel (FC-2b) and curcumin powder-incorporated gel (FC-1) are shown in Figure 7. After 7 h, curcumin permeated from FC-1 and FC-2b was 38.17% and 60.29%, respectively. Thus, the FC-2 gel showed about 28% increase in the drug permeation when compared to FC-1. This indicates that the permeation of curcumin was enhanced from nanocrystals due to its enhanced dissolution in the aqueous gel base [46]. Studies have suggested that nanocrystals are known to deposit in the dermis layer of the skin due to increased skin permeation when compared to standard topical formulations. In the latter case, the released drug tends to stay in the epidermis [47]. The greater skin permeation by the nanocrystals can also be attributed to their smaller size

compared to the unprocessed curcumin powder. The other major formulation parameters that affect nanocrystal penetration efficiency are the viscosity, lipophilicity and polarity of the vehicle selected [48]. Carbopol gels are sufficiently polar to enable the dissolution of the curcumin nanocrystals.

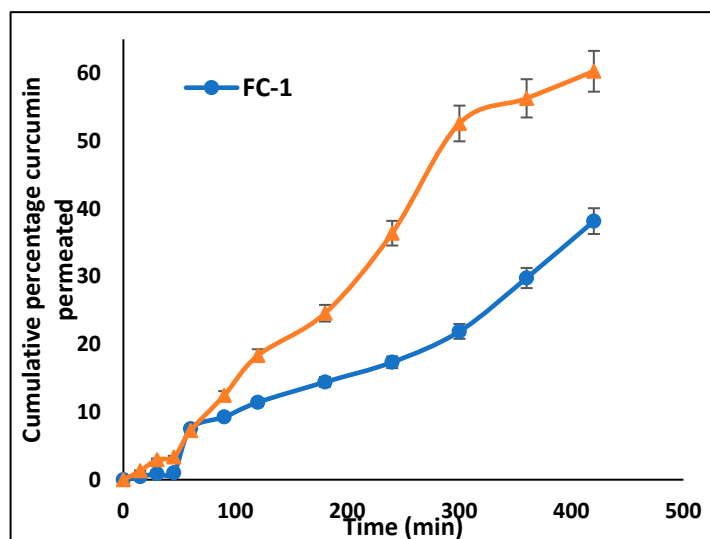


**Figure 7.** Ex vivo permeation of curcumin from FC-1 and FC-2b through excised rat skin. FC-1: Unprocessed curcumin powder-containing gel (1.0% w/w); FC-2b: Curcumin nanocrystal-containing gel (1.0% w/w).

### 3.6.3. In Vivo Skin Irritability Study

The skin irritation potential of FC-2b was studied in healthy Albino Wistar rats by application onto their intact skin. This investigation was necessary since the semi-crystalline nature of the nanocrystals can produce a particular degree of skin irritation on application and more so if applied to wounds. The formulations were applied to the rats' shaven dorsal surfaces as shown in Figure 8. The nanocrystal gel was compatible with rat skin and showed no irritation on visual inspection. The rats were observed for any signs of erythema or oedema after 0, 24, and 72 h. There was no indication of erythema or oedema formation in any of the groups throughout the 72 h study period. The average skin irritation index was calculated to be 0. From the results, it can be concluded that curcumin nanocrystal gel was found to be irritation-free, like the marketed formulation (Povidone ointment) [49].

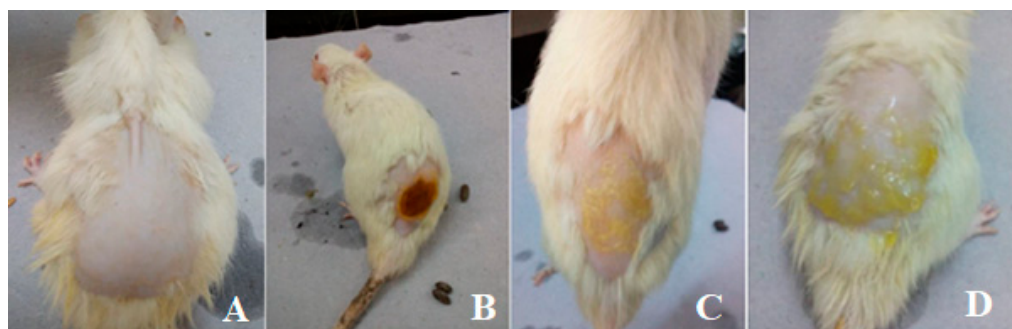


**Figure 8.** Images showing application of treatments for skin irritation studies: (A) Group I is the control or untreated; (B) Group II received the standard or Povidone Iodine Ointment USP, 5.0% w/w; (C) Group III received FC-1 or 1% unprocessed curcumin powder-containing gel; (D) Group IV received FC-2b or curcumin nanocrystal gel, 1.0% w/w.

#### 3.6.4. Excision Wound Healing Study

In the present study, an excision wound model was chosen and animals were divided into five groups of six animals each. All animals were treated as per the procedure given in the methodology. The wound area was checked at 1st, 4th, 7th, 10th, 15th, and 20th days. Wound contraction started at the 4th day of the study. On the 15th day, the healed wound structure showed normal epithelization, restoration of adnexa, and fibrosis within the dermis in Groups II-V. At the same time, the control group lagged behind the treated groups in the occurrence of the amount of ground substance in the granulation tissue. At the end of the 20th day, Group V showed the quickest healing compared to all other groups, including the standard, with a wound contraction of 99.80%. These differences can be observed in the images shown in Figure 9. The percentage contraction of wounds on the 20th day was significantly greater with a  $p < 0.05$  in Group V when compared to Groups I, III and IV (Figure 10). Interestingly, Group V showed a healing rate better than that of the standard (Group II) although both started at the same pace at the beginning of the study. Between Group III and Group V, the latter showed a 20% increase in wound contraction at the end of 20 days. This faster wound contraction and healing in this treatment group was due to the rapid solubilizing effect of curcumin crystals and permeation into the tissues. The nanosize of the crystals was responsible for their rapid dissolution in the gel base, which would not have been possible for the relatively larger particle size of the plain curcumin powder (FC-1) [45]. It was observed that the rate of wound healing was also significant ( $p < 0.05$ ) in Group IV when compared to Group I and II for the same reason. As expected, using a higher strength of curcumin nanocrystals of 1.0% w/w in gel also made a difference to the percentage of wound contraction when comparing Group V to Group IV which received 0.5% w/w. Figure 10 shows the change in the contraction of the wounds between different treatment groups from the first to the 20th day since inflicting the wounds in the animals. The control group and Group III showed the slowest wound contraction during the period of 20 days.

As explained earlier, the wound healing effects of curcumin are credited to its antioxidant, anti-inflammatory and antimicrobial properties. Several studies report that topical application of curcumin to normal and burn wounds promotes healing by increasing epithelial regeneration, collagen deposition, the proliferation of fibroblasts, increased vascular density, and wound contraction [4,50,51].

Conclusively, nanocrystals of curcumin were more efficient in wound healing than unprocessed or raw curcumin. This fact further confirms that the particle size in nano dimensions and, consequently, the high surface area-to-volume play important roles in intimate wound interaction and easy permeation into the wound site [48]. In addition, it is possible that nanocrystals can provide a sustained and controlled release of the drug at the wound site.

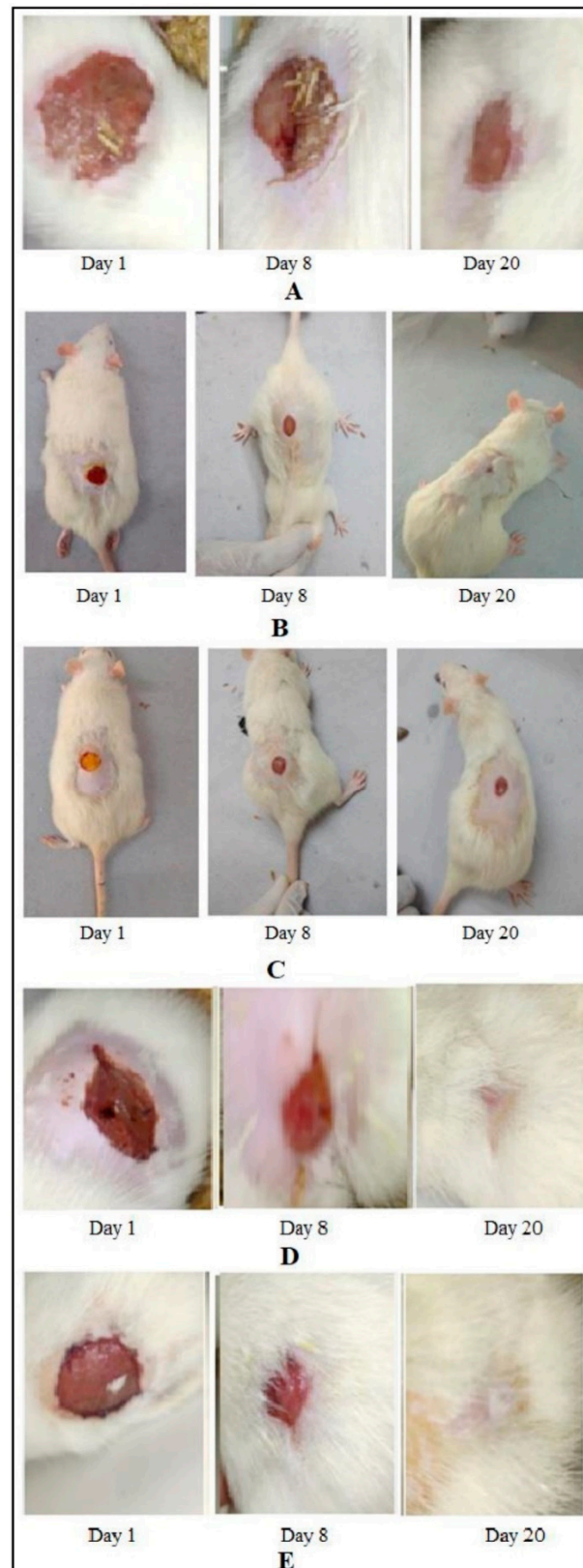


**Figure 9.** Images from excision wound healing studies taken after the 1st, 8th and 20th day. (A) Group I or Control was untreated. (B) Group II or standard received Povidone Iodine ointment USP (5% w/w). (C) Group III received FC-1 or 1% w/w unprocessed curcumin powder-containing gel. (D) Group IV received FC-2a or 0.5% w/w curcumin nanocrystal gel. (E) Group V received FC-2b or 1.0% w/w curcumin nanocrystal gel.

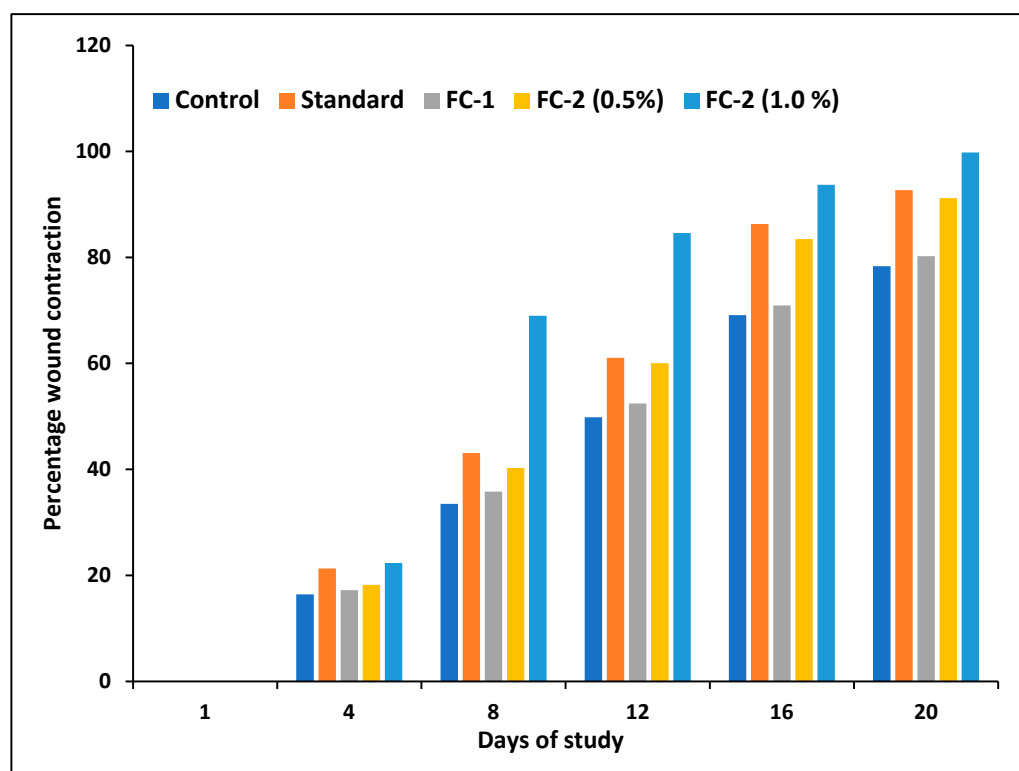


**Figure 10.** Change in percentage contraction of wound with time in different groups. Control: Untreated; Standard: Povidone Iodine ointment USP; FC-1: 1% unprocessed curcumin powder-containing gel, FC-2 (0.5%): 0.5% curcumin nanocrystal containing gel; FC-2 (1.0%): 0.5% curcumin nanocrystal containing gel.

#### 4. Conclusions

Although therapeutics from herbal sources are popular for their safety and mild properties, physicochemical properties such as solubility and permeability can significantly impact their effectiveness. The employment of solubility-enhancing techniques such as nanocrystallization or sonoprecipitation can substantially improve the topical availability of poorly aqueous soluble curcumin. This study shows that it is possible to develop a topical formulation consisting of curcumin nanocrystals in a carbopol gel base to heal burns or other dermal wounds rapidly. The formulation was also free of skin irritation potential and can be considered promising as an effective and safe alternative to commercially available gels or ointments. Future work may involve studying the optimized formulation concerning detailed preclinical toxicity and efficacy study. It may also require clinical evaluation of the optimized formulation. However, the scale-up of the process and large-scale production of the nanocrystals is always challenging, which can be overcome by adopting advanced technologies such as high-pressure homogenization, and large-scale probe sonicators, among others.

**Author Contributions:** Conceptualization, M.K. and S.M.; data curation, V.K. and M.K.; investigation, V.K.; methodology, V.K. and M.K.; resources, M.K.; software, V.K.; supervision, S.M.; validation, V.K. and S.M.; visualization, M.K. and S.M.; writing—original draft, M.K.; writing—review & editing, M.K. and S.M. All authors have read and agreed to the published version of the manuscript.

**Funding:** This research received no external funding.

**Institutional Review Board Statement:** The study was conducted in accordance with the Declaration of Helsinki, and approved by the Institutional Animal Ethics Committee of NGSM Institute of Pharmaceutical Sciences (protocol code: NGSM/IAEC/2018-19/82 and date of approval: 12 July 2018).

**Data Availability Statement:** Not applicable.

**Acknowledgments:** The authors would like to thank the Nitte (Deemed to be University) and NGSM Institute of Pharmaceutical Sciences (NGSMIPS) for providing the laboratory facilities and material support.

**Conflicts of Interest:** The authors declare no conflict of interest.

## References

1. Boer, M.; Duchnik, E.; Maleszka, R.; Marchlewicz, M. Structural and Biophysical Characteristics of Human Skin in Maintaining Proper Epidermal Barrier Function. *Postep. Dermatol. I Alergol.* **2016**, *33*, 1–5. [[CrossRef](#)] [[PubMed](#)]
2. Ansari, P.; Akther, S.; Hannan, J.M.A.; Seidel, V.; Nujat, N.J.; Abdel-Wahab, Y.H.A. Pharmacologically Active Phytomolecules Isolated from Traditional Antidiabetic Plants and Their Therapeutic Role for the Management of Diabetes Mellitus. *Molecules* **2022**, *27*, 4278. [[CrossRef](#)] [[PubMed](#)]
3. Gandhi, P.; Khan, Z.; Chakraverty, N. Soluble Curcumin: A Promising Oral Supplement for Health Management. *J. Appl. Pharm. Sci.* **2011**, *1*, 1–7.
4. Akbik, D.; Ghadiri, M.; Chrzanowski, W.; Rohanizadeh, R. Curcumin as a Wound Healing Agent. *Life Sci.* **2014**, *116*, 1–7. [[CrossRef](#)]
5. Mohanty, C.; Sahoo, S.K. The in Vitro Stability and in Vivo Pharmacokinetics of Curcumin Prepared as an Aqueous Nanoparticulate Formulation. *Biomaterials* **2010**, *31*, 6597–6611. [[CrossRef](#)]
6. Merisko-Liversidge, E.; Liversidge, G.G.; Cooper, E.R. Nanosizing: A Formulation Approach for Poorly-Water-Soluble Compounds. *Eur. J. Pharm. Sci.* **2003**, *18*, 113–120. [[CrossRef](#)]
7. Fu, Q.; Sun, J.; Ai, X.; Zhang, P.; Li, M.; Wang, Y.; Liu, X.; Sun, Y.; Sui, X.; Sun, L.; et al. Nimodipine Nanocrystals for Oral Bioavailability Improvement: Role of Mesenteric Lymph Transport in the Oral Absorption. *Int. J. Pharm.* **2013**, *448*, 290–297. [[CrossRef](#)]
8. Gigliobianco, M.R.; Casadidio, C.; Censi, R.; Di Martino, P. Nanocrystals of Poorly Soluble Drugs: Drug Bioavailability and Physicochemical Stability. *Pharmaceutics* **2018**, *10*, 134. [[CrossRef](#)]
9. Kalia, Y.N.; Guy, R.H. Modeling Transdermal Drug Release. *Adv. Drug Deliv. Rev.* **2001**, *48*, 159–172. [[CrossRef](#)]
10. Carneiro, R.d.S.; Canuto, M.R.; Ribeiro, L.K.; Ferreira, D.C.L.; Assunção, A.F.C.; Costa, C.A.C.B.; de Freitas, J.D.; Rai, M.; Cavalcante, L.S.; Alves, W.d.S.; et al. Novel Antibacterial Efficacy of ZnO Nanocrystals/Ag Nanoparticles Loaded with Extract of *Ximenia Americana* L. (Stem Bark) for Wound Healing. *S. Afr. J. Bot.* **2022**, *151*, 18–32. [[CrossRef](#)]
11. Ouyang, X.K.; Zhao, L.; Jiang, F.; Ling, J.; Yang, L.Y.; Wang, N. Cellulose Nanocrystal/Calcium Alginate-Based Porous Microspheres for Rapid Hemostasis and Wound Healing. *Carbohydr. Polym.* **2022**, *293*, 119688. [[CrossRef](#)] [[PubMed](#)]
12. Koseki, Y.; Ikuta, Y.; Taemaitree, F.; Saito, N.; Suzuki, R.; Dao, A.T.N.; Onodera, T.; Oikawa, H.; Kasai, H. Fabrication of Size-Controlled SN-38 Pure Drug Nanocrystals through an Ultrasound-Assisted Reprecipitation Method toward Efficient Drug Delivery for Cancer Treatment. *J. Cryst. Growth* **2021**, *572*, 126265. [[CrossRef](#)]
13. Heng, M.C. Topical Curcumin: A Review of Mechanisms and Uses in Dermatology. *Int. J. Dermatol. Clin. Res.* **2017**, *3*, 010–017. [[CrossRef](#)]
14. Parmar, P.K.; Wadhawan, J.; Bansal, A.K. Pharmaceutical Nanocrystals: A Promising Approach for Improved Topical Drug Delivery. *Drug Discov. Today* **2021**, *26*, 2329–2349. [[CrossRef](#)] [[PubMed](#)]
15. Poojary, K.K.; Nayak, G.; Vasani, A.; Kumari, S.; Dcunha, R.; Kunhiraman, J.P.; Gopalan, D.; Rao, R.R.; Mutalik, S.; Kalthur, S.G.; et al. Curcumin Nanocrystals Attenuate Cyclophosphamide-Induced Testicular Toxicity in Mice. *Toxicol. Appl. Pharmacol.* **2021**, *433*, 115772. [[CrossRef](#)]
16. Zong, R.; Ruan, H.; Zhu, W.; Zhang, P.; Feng, Z.; Liu, C.; Fan, S.; Liang, H.; Li, J. Curcumin Nanocrystals with Tunable Surface Zeta Potential: Preparation, Characterization and Antibacterial Study. *J. Drug. Deliv. Sci. Technol.* **2022**, *76*, 103771. [[CrossRef](#)]
17. Finnegan, S.; Percival, S.L. Clinical and Antibiofilm Efficacy of Antimicrobial Hydrogels. *Adv. Wound Care* **2015**, *4*, 398. [[CrossRef](#)]
18. Islam, M.T.; Rodríguez-Hornedo, N.; Ciotti, S.; Ackermann, C. Rheological Characterization of Topical Carbomer Gels Neutralized to Different PH. *Pharm. Res.* **2004**, *21*, 1192–1199. [[CrossRef](#)]
19. Shelake, S.S.; Patil, S.V.; Patil, S.S.; Sangave, P. Formulation and Evaluation of Fenofibrate-Loaded Nanoparticles by Precipitation Method. *Indian J. Pharm. Sci.* **2018**, *80*, 420–427. [[CrossRef](#)]
20. De Waard, H.; Frijlink, H.W.; Hinrichs, W.L.J. Bottom-Up Preparation Techniques for Nanocrystals of Lipophilic Drugs. *Pharm. Res.* **2011**, *28*, 1220. [[CrossRef](#)]
21. Khan, S.; Matas, M.D.; Zhang, J.; Anwar, J. Nanocrystal Preparation: Low-Energy Precipitation Method Revisited. *Crystal Growth and Design* **2013**, *13*, 2766–2777. [[CrossRef](#)]
22. Abdelwahed, W.; Degobert, G.; Stainmesse, S.; Fessi, H. Freeze-Drying of Nanoparticles: Formulation, Process and Storage Considerations. *Adv. Drug Deliv. Rev.* **2006**, *58*, 1688–1713. [[CrossRef](#)] [[PubMed](#)]
23. Zhai, X.; Lademann, J.; Keck, C.M.; Müller, R.H. Nanocrystals of Medium Soluble Actives—Novel Concept for Improved Dermal Delivery and Production Strategy. *Int. J. Pharm.* **2014**, *470*, 141–150. [[CrossRef](#)] [[PubMed](#)]
24. Kaszuba, M.; Corbett, J.; Watson, F.M.N.; Jones, A. High-Concentration Zeta Potential Measurements Using Light-Scattering Techniques. *Philos. Trans. R. Soc. A Math. Phys. Eng. Sci.* **2010**, *368*, 4439. [[CrossRef](#)]

25. Marković, Z.M.; Prekodravac, J.R.; Tošić, D.D.; Holclajtner-Antunović, I.D.; Milosavljević, M.S.; Dramićanin, M.D.; Todorović-Marković, B.M. Facile Synthesis of Water-Soluble Curcumin Nanocrystals. *J. Serb. Chem. Soc.* **2015**, *80*, 63–72. [[CrossRef](#)]
26. Agrawal, R.; Sandhu, S.K.; Sharma, I.; Kaur, I.P. Development and Evaluation of Curcumin-Loaded Elastic Vesicles as an Effective Topical Anti-Inflammatory Formulation. *AAPS PharmSciTech* **2015**, *16*, 364. [[CrossRef](#)]
27. Zhai, X.; Lademann, J.; Keck, C.M.; Müller, R.H. Dermal Nanocrystals from Medium Soluble Actives—Physical Stability and Stability Affecting Parameters. *Eur. J. Pharm. Biopharm.* **2014**, *88*, 85–91. [[CrossRef](#)]
28. Zamarioli, C.M.; Martins, R.M.; Carvalho, E.C.; Freitas, L.A.P. Nanoparticles Containing Curcuminoids (*Curcuma longa*): Development of Topical Delivery Formulation. *Rev. Bras. Farmacogn.* **2015**, *25*, 53–60. [[CrossRef](#)]
29. Mutalik, S.; Suthar, N.A.; Managuli, R.S.; Shetty, P.K.; Avadhani, K.; Kalthur, G.; Kulkarni, R.V.; Thomas, R. Development and Performance Evaluation of Novel Nanoparticles of a Grafted Copolymer Loaded with Curcumin. *Int. J. Biol. Macromol.* **2016**, *86*, 709–720. [[CrossRef](#)]
30. Gong, C.Y.; Wu, Q.J.; Wang, Y.J.; Zhang, D.D.; Luo, F.; Zhao, X.; Wei, Y.Q.; Qian, Z.Y. A Biodegradable Hydrogel System Containing Curcumin Encapsulated in Micelles for Cutaneous Wound Healing. *Biomaterials* **2013**, *34*, 6377–6387. [[CrossRef](#)]
31. Patel, N.A.; Patel, N.J.; Patel, R.P. Formulation and Evaluation of Curcumin Gel for Topical Application. *Pharm. Dev. Technol.* **2009**, *14*, 83–92. [[CrossRef](#)] [[PubMed](#)]
32. Estevão, L.R.d.M.; Cassini-Vieira, P.; Leite, A.G.B.; Bulhões, A.A.V.d.C.; Barcelos, L.d.S.; Evêncio-Neto, J. Morphological Evaluation of Wound Healing Events in the Excisional Wound Healing Model in Rats. *Bio-Protoc.* **2019**, *9*, e3285. [[CrossRef](#)] [[PubMed](#)]
33. Agarwal, P.K.; Singh, A.; Gaurav, K.; Goel, S.; Khanna, H.D.; Goel, R.K. Evaluation of Wound Healing Activity of Extracts of Plantain Banana (*Musa Sapientum* Var. *Paradisiaca*) in Rats. Available online: <https://pubmed.ncbi.nlm.nih.gov/19317349/> (accessed on 16 September 2022).
34. Jain, S.; Patel, K.; Arora, S.; Reddy, V.A.; Dora, C.P. Formulation, Optimization, and in Vitro-in Vivo Evaluation of Olmesartan Medoxomil Nanocrystals. *Drug Deliv. Transl. Res.* **2017**, *7*, 292–303. [[CrossRef](#)] [[PubMed](#)]
35. Bonaccorso, A.; Gigliobianco, M.R.; Pellitteri, R.; Santonocito, D.; Carbone, C.; Di Martino, P.; Puglisi, G.; Musumeci, T. Optimization of Curcumin Nanocrystals as Promising Strategy for Nose-to-Brain Delivery Application. *Pharmaceutics* **2020**, *12*, 476. [[CrossRef](#)] [[PubMed](#)]
36. El-Batal, A.I.; Elmenshawi, S.F.; Abdelhaleem Ali, A.M.; Eldbaiky, E.G. Preparation and Characterization of Silymarin Nanocrystals and Phytosomes with Investigation of Their Stability Using Gamma Irradiation. *Indian J. Pharm. Educ. Res.* **2018**, *52*, S174–S183. [[CrossRef](#)]
37. Pawar, Y.B.; Purohit, H.; Valicherla, G.R.; Munjal, B.; Lale, S.V.; Patel, S.B.; Bansal, A.K. Novel Lipid Based Oral Formulation of Curcumin: Development and Optimization by Design of Experiments Approach. *Int. J. Pharm.* **2012**, *436*, 617–623. [[CrossRef](#)] [[PubMed](#)]
38. Yue, P.; Zhou, W.; Huang, G.; Lei, F.; Chen, Y.; Ma, Z.; Chen, L.; Yang, M. Nanocrystals Based Pulmonary Inhalation Delivery System: Advance and Challenge. *Drug Deliv.* **2022**, *29*, 637. [[CrossRef](#)]
39. Homayouni, A.; Amini, M.; Sohrabi, M.; Varshosaz, J.; Nokhodchi, A. Curcumin Nanoparticles Containing Poloxamer or Soluplus Tailored by High Pressure Homogenization Using Antisolvent Crystallization. *Int. J. Pharm.* **2019**, *562*, 124–134. [[CrossRef](#)]
40. Yadav, D.; Kumar, N. Nanonization of Curcumin by Antisolvent Precipitation: Process Development, Characterization, Freeze Drying and Stability Performance. *Int. J. Pharm.* **2014**, *477*, 564–577. [[CrossRef](#)]
41. Homayouni, A.; Sohrabi, M.; Amini, M.; Varshosaz, J.; Nokhodchi, A. Effect of High Pressure Homogenization on Physicochemical Properties of Curcumin Nanoparticles Prepared by Antisolvent Crystallization Using HPMC or PVP. *Mater. Sci. Eng. C Mater. Biol. Appl.* **2019**, *98*, 185–196. [[CrossRef](#)]
42. Londoño-Restrepo, S.M.; Jeronimo-Cruz, R.; Millán-Malo, B.M.; Rivera-Muñoz, E.M.; Rodriguez-García, M.E. Effect of the Nano Crystal Size on the X-Ray Diffraction Patterns of Biogenic Hydroxyapatite from Human, Bovine, and Porcine Bones. *Sci. Rep.* **2019**, *9*, 5915. [[CrossRef](#)]
43. Chu, K.R.; Lee, E.; Jeong, S.H.; Park, E.S. Effect of Particle Size on the Dissolution Behaviors of Poorly Water-Soluble Drugs. *Arch. Pharm. Res.* **2012**, *35*, 1187–1195. [[CrossRef](#)]
44. Dizaj, S.M.; Vazifehasl, Z.; Salatin, S.; Adibkia, K.; Javadzadeh, Y. Nanosizing of Drugs: Effect on Dissolution Rate. *Res. Pharm. Sci.* **2015**, *10*, 95. [[PubMed](#)]
45. Shi, Z.; Pan, S.; Wang, L.; Li, S. Topical Gel Based Nanoparticles for the Controlled Release of Oleanolic Acid: Design and in Vivo Characterization of a Cubic Liquid Crystalline Anti-Inflammatory Drug. *BMC Complement. Med. Ther.* **2021**, *21*, 224. [[CrossRef](#)] [[PubMed](#)]
46. Kumar, M.; Shanthi, N.; Mahato, A.K.; Soni, S.; Rajnikanth, P.S. Preparation of Luliconazole Nanocrystals Loaded Hydrogel for Improvement of Dissolution and Antifungal Activity. *Heliyon* **2019**, *5*, e01688. [[CrossRef](#)] [[PubMed](#)]
47. Pyo, S.M.; Hespeler, D.; Keck, C.M.; Müller, R.H. Dermal Miconazole Nitrate Nanocrystals—Formulation Development, Increased Antifungal Efficacy & Skin Penetration. *Int. J. Pharm.* **2017**, *531*, 350–359. [[CrossRef](#)]
48. Pelikh, O.; Keck, C.M. Hair Follicle Targeting and Dermal Drug Delivery with Curcumin Drug Nanocrystals—Essential Influence of Excipients. *Nanomaterials* **2020**, *10*, 2323. [[CrossRef](#)]
49. Tirunagari, M.; Jangala, V.R.; Nandagopal, A. Development and Physicochemical, In Vitro and In Vivo Evaluation of Transdermal Patches of Zaleplon. *Indian J. Pharm. Educ. Res.* **2013**, *47*, 49–58. [[CrossRef](#)]

- 
50. Sidhu, G.S.; Singh, A.K.; Thaloor, D.; Banaudha, K.K.; Patnaik, G.K.; Srimal, R.C.; Maheshwari, R.K. Enhancement of Wound Healing by Curcumin in Animals. *Wound Repair Regen.* **1998**, *6*, 167–177. [[CrossRef](#)]
  51. Mehrabani, D.; Farjam, M.; Geramizadeh, B.; Tanideh, N.; Amini, M.; Panjehshahin, M.R. The Healing Effect of Curcumin on Burn Wounds in Rat. *World J. Plast. Surg.* **2015**, *4*, 29.